Journal for ImmunoTherapy of Cancer

ICOS-expressing CAR-T cells mediate durable eradication of triple-negative breast cancer and metastasis

Lixue Cao ,[1] Haojie Peng,[2,3] Yanzhen Chen,[4] Baijin Xia,[1,5] Tao Zeng,[2] Jialing Guo,[1] Fei Yu ,[1] Haiyan Ye,[4] Hui Zhang ,[6] Xinxin Chen [2]

To cite: Cao L, Peng H, Chen Y, *et al*. ICOS-expressing CAR-T cells mediate durable eradication of triple-negative breast cancer and metastasis. *Journal for ImmunoTherapy of Cancer* 2024;**12**:e010028. doi:10.1136/jitc-2024-010028

► Additional supplemental material is published online only. To view, please visit the journal online (https://doi.org/10.1136/jitc-2024-010028).

LC, HP, YC and BX contributed equally.

Received 08 July 2024

Accepted 17 October 2024

For numbered affiliations see end of article.

Correspondence to
Xinxin Chen;
chenxinxin@gzhmu.edu.cn

Hui Zhang;
zhangh92@mail.sysu.edu.cn

Haiyan Ye;
yehaiyan@gdph.org.cn

Fei Yu; yufei@gdph.org.cn

ABSTRACT

Background The failure of conventional therapies and the propensity for recurrence and metastasis make triple-negative breast cancer (TNBC) a formidable challenge with grim prognoses and diminished survival rates. Immunotherapy, including immune checkpoint blockade and chimeric antigen receptor (CAR)-T cell therapy, presents innovative and potentially more effective strategies for addressing TNBC. Within this context, the inducible costimulator (ICOS), a member of the CTLA4/CD28 family, plays a crucial role in regulating immune responses and T-cell differentiation by binding to its ligand ICOSL. However, the impact of the ICOS/ICOSL axis on cancer varies.

Methods In this study, immunohistochemistry was conducted to examine the expression level of ICOSL in TNBC tumor tissues. We developed ICOS-enhanced B7H3-CAR-T cells (ICOS-B7H3-CAR) using the third-generation CAR-T cell technology, which featured magnified ICOS expression and targeted the B7H3 antigen. Xenograft and metastasis models of TNBC were conducted to examine the cytotoxicity and durability of CAR-T cells in tumors. Overexpression and CRISPR/Cas9-mediated knockout (KO) techniques were employed to regulate the expression of ICOSL on TNBC cell lines.

Results Notably, we observed elevated ICOSL expression in TNBC tumor tissues, which correlated with poor survival prognosis in patients with TNBC. Compared with conventional B7H3-CAR-T cells, ICOS-B7H3-CAR-T cells significantly inhibited the tumor growth of TNBC cells both in vitro and in vivo, accompanied by increased secretion of cytokines such as interferon gamma and tumor necrosis factor alpha. Furthermore, the in vivo experiments illustrated that ICOS-B7H3-CAR-T cells exhibited prolonged antitumor activity and could effectively eradicate metastases in a TNBC metastasis model, consequently extending survival. Importantly, manipulating the expression of ICOSL on TNBC cells through overexpression or KO significantly influenced the function of ICOS-B7H3-CAR-T cells. This suggests that the level of ICOSL expression on TNBC cells is critical for enhancing the potent antitumor effects of ICOS-B7H3-CAR-T cells.

Conclusion Overall, our study highlights the potential clinical application of ICOS as a promising strategy for combating TNBC recurrence and metastasis.

WHAT IS ALREADY KNOWN ON THIS TOPIC

⇒ The success of blocking antibodies targeting CTLA-4 and programmed death receptor 1 in clinic, such as ipilimumab, pembrolizumab, and nivolumab, has aroused excitement due to their notable regression of melanoma and other cancers. Inducible costimulator (ICOS), a member of the CTLA4/CD28 family, displays promise as a costimulatory target for immunotherapy. However, its effectiveness in combination with other agents like the anti-CTLA-4 antibody (tremelimumab) in solid tumors remains limited. The impact of ICOS/ICOS ligand (ICOSL) on cancer outcomes varies depending on the dominant cell type involved.

WHAT THIS STUDY ADDS

⇒ Our study developed ICOS-B7H3-chimeric antigen receptor (CAR)-T cells with enhanced ICOS expression targeting the B7H3 antigen. These CAR-T cells exhibited prolonged antitumor activity, effectively eliminating metastases in vitro and in vivo, and increased cytokine secretion. Modulating ICOSL expression on triple-negative breast cancer (TNBC) cells significantly influenced the function of ICOS-B7H3-CAR-T cells, emphasizing its importance for their superior antitumor effects.

HOW THIS STUDY MIGHT AFFECT RESEARCH, PRACTICE OR POLICY

⇒ The findings of this study indicate that ICOS has significant potential in enhancing the cytotoxicity and durability of CAR-T cells. This represents a promising approach for combating recurrence and metastasis in TNBC.

INTRODUCTION

Triple-negative breast cancer (TNBC) is the most complex and challenging subtype of breast cancer, defined by the absence of three key receptors: estrogen receptor, progesterone receptor (PR), and human epidermal growth factor receptor 2 (HER2).[1] TNBC poses challenges for conventional therapies, such as surgical resection, radiation, and neoadjuvant chemotherapy.[2] These treatments often fail to achieve complete eradication, leading

to systemic recurrence and metastasis and frequently contribute to a grim prognosis and diminished survival rates.[2] Immune checkpoint blockade (ICB), such as programmed death receptor 1 inhibitors in combination with chemotherapy, has demonstrated significant efficacy in clinical trials, which have been approved for application in patients with early-stage TNBC and programmed death-ligand 1$^+$ metastatic TNBC.[3 4] However, the rates of pathological complete response (pCR) are as low as 25% in non-immune-enriched TNBC with ICB treatment, compared with 75% in immune-enriched TNBC with ICB treatment (NCT02883062).[3] Hence, these findings underscore the pressing need for innovative and more effective therapeutic strategies in tackling TNBC, particularly in the context of non-immune-enriched subtypes.

Currently, chimeric antigen receptor (CAR) T therapy, as a form of immunotherapy, redirects the patient's immune response to identify and eliminate tumor cells expressing tumor-associated antigens (TAAs), providing a promising avenue for treating TNBC.[5–7] Multiple potential TAAs have been validated in TNBC, such as mesothelin, folate receptor-alpha, tumor endothelial marker 8, NKG2D ligands, epidermal growth factor receptor (EGFR) and CD276 molecule (B7-H3), which exert antitumor effects of CAR-T against TNBC tumors.[5–11] However, the effectiveness of CAR-T cell therapy against solid tumors is limited, largely attributed to tumor-induced immunosuppression.[12] CAR-T cell therapy's effectiveness might be improved by using agents that make tumor cells more susceptible to T-cell attack, such as cytokines and inhibitors.[13 14] For example, the TGF-β-receptor I kinase inhibitor boosts the tumor-fighting efficacy of ROR1-CAR-T cells directed against TNBC in both two dimensional in vitro culture and a microphysiologic three dimensional tumor model by alleviating CAR-T cells exhaustion.[13] In TNBC models, the combination of a CDK7 inhibitor with EGFR CAR-T cell therapy reduced immune resistance, inhibited tumor growth, and suppressed metastasis.[14] However, the effectiveness of these approaches in enhancing antitumor activity in patients remains uncertain. Consequently, there is a pressing need for additional strategies to augment the efficacy of CAR-T cells against solid tumors.

Inducible costimulator ligand (ICOSL) is highly expressed in solid tumor cells, such as melanoma and rhabdomyosarcoma, and is associated with poor prognosis.[15 16] Inducible T cell costimulator (ICOS), which belongs to the CD28 family, is upregulated on T cell activation.[17] Through interaction with its ligand, ICOSL, ICOS plays a pivotal role in shaping subsequent T cell differentiation and promoting their survival, a function distinct from that of CD28.[17] This interaction stimulates T cells to generate a range of cytokines, such as interleukin (IL)-10, IL-4, IL-5, IFN-γ, and IL-17, with the predominant effect varying depending on the specific cell type involved.[15] High expression of ICOS on follicular helper T cells (TFH) promotes the proliferation and differentiation of B cells into plasma cells through interactions with ICOSL, which is crucial for the T cell-dependent B cell response within germinal centers (GCs).[18] Recently, accumulating evidence have highlighted the role of ICOS/ICOSL in shaping the tumor immune environment across various cancers, including melanoma, colorectal cancer, ovarian cancer, and breast cancer.[15 19–22] However, the impact of ICOS/ICOSL on cancer varies, depending on the dominant cell type involved.[15] For example, in colorectal cancer, ICOS expression correlates positively with prognosis, resembling characteristics of Th1 and cytotoxic T cells.[20] Conversely, tumor-infiltrating ICOS$^+$ regulatory T cells (Tregs) serve as a negative prognostic factor in ovarian cancer and breast cancer, as they bind to ICOSL$^+$ plasmacytoid dendritic cells (pDCs), fostering a tumor-repressive environment through IL-10 secretion.[21 22] Therefore, further examination is needed to assess the clinical application of ICOS/ICOSL in cancer therapy.

Several studies have demonstrated that ICOS could enhance CAR-T immunotherapy.[23–25] For instance, a CAR incorporating the ICOS transmembrane domain (TMD) strengthens interactions between T cells and antigen-presenting target cells but does not support TFH development or GC formation in vivo.[25] Additionally, an ICOS-based CAR that includes both the TMD and intracellular domain (ICD) promotes the development of bipolar Th17/Th1 cells, resulting in enhanced effector function and improved persistence in vivo.[23] In this study, we observed high expression of ICOSL in TNBC tumor tissue, correlating with poor prognostic survival in patients with TNBC. Consequently, we developed ICOS-B7H3-CAR-T cells incorporating full length of ICOS, which featured enhanced ICOS expression and targeted B7H3. This modification improves CAR-T cell efficacy by enabling binding to ICOSL on tumor cells, which enhances both CAR-T cell proliferation and persistence. Compared with B7H3-CAR-T cells, ICOS-B7H3-CAR-T cells demonstrated heightened antitumor activity against TNBC cells both in vitro and in vivo. Additionally, ICOS-B7H3-CAR-T cells increased the secretion of cytokines such as interferon gamma (IFN-γ) and tumor necrosis factor alpha (TNF-α). Moreover, in vivo experiments revealed that ICOS-B7H3-CAR-T cells displayed prolonged antitumor activity and could effectively eliminate metastases in a TNBC metastasis model. Our findings suggest that the expression of ICOSL on TNBC cells enhances the superior effect of ICOS-B7H3-CAR-T cells. Thus, targeting ICOS-expressing CAR-T cells may represent a promising strategy for combating TNBC recurrence and metastasis.

MATERIALS AND METHODS

Cell lines

The HEK293T human embryonic kidney cell line and TNBC cell lines MDA-MB-231, Hs578T, MDA-MB-468, HCC1937, and MDA-MB-436 were obtained from American Type Culture Collection (Manassas, Virginia, USA).

Cells were cultured in Dulbecco's Modified Eagle's Medium (Gibco) with 10% fetal bovine serum and 1% penicillin-streptomycin at 37°C with 5% CO2. Mycoplasma tests were negative, and short tandem repeats analysis authenticated all cell lines.

Purification and culture of primary human CD8+ T lymphocytes

Peripheral blood samples were collected from healthy donors recruited at the Second Affiliated Hospital of Guangzhou Medical University. These samples were anonymized in accordance with local ethical guidelines and the Declaration of Helsinki. Primary human CD8+ T cells were isolated from peripheral blood mononuclear cells using the EasySep Human CD8 Positive Selection Kit (Cat No. 17853, STEMCELL, Canada) following manufacturer instructions. The purified CD8+ T lymphocytes were activated with 2 µg/mL anti-CD3 Ab (Cat No. 317326, BioLegend, San Diego, California, USA) and 1 µg/mL anti-CD28 Ab (Cat No. 302934, BioLegend) and supplemented with 10 ng/mL recombinant hIL-2 (Cat No. BT-002–050, R&D Systems, Minneapolis, Minnesota, USA) every 3 days.

Construction of lentiviral vector

The anti-B7H3 single-chain variable fragment (scFv) was derived from mAb 376.96[26 27] and fused with the endodomains of CD28 (NM_006139.3), CD137 (NM_001561.5), and CD3ζ (NM_198053.2) to construct B7H3-specific CAR-T cells. As mock CAR-T cells, GP120-CAR targets the gp120 antigen of HIV-1 using sequences from a prior study.[28] Lentiviral vectors carrying the B7H3-specific CAR were modified with a FLAG tag for western blot detection. Full-length human ICOS (NM_012092.4) was PCR-amplified from a custom complementary DNA clone purchased from Beijing Tsingke Biotech. ICOS-B7H3 CAR constructs were created by fusing ICOS gene fragments with a T2A self-cleaving peptide into the CAR-containing viral vector. CAR plasmids included P2A self-cleaving peptide fused with truncated CD19. The human ICOSL gene (NM_001283050.2) was generated to pLVX-IRES-Puro vector. Lentiviral-based CRISPR/Cas9 technology was used to knockout (KO) ICOSL in MDA-MB-231 cells, employing a small guide RNA (sgRNA) sequence (5'-GAGAAGGAAGTCAGAGCGA-3') cloned into the LentiCRISPR-v2 vector.[29]

Transduction of recombinant lentiviral particles

Plasmids encoding various CAR moieties, pMD2.G (VSV-G envelope), and the packaging vector psPAX2 were cotransfected into HEK293T cells using EndoFectin MAX transfection reagent (Cat No. EF001, GeneCopoeia, Guangzhou, Guangdong, China). Activated CD8+ T lymphocytes were transduced with lentiviral supernatant supplemented with 8 µg/mL polybrene (Sigma-Aldrich, Saint Louis, Missouri, USA) and centrifuged at 350×g at 37°C for 90 min. MDA-MB-231 and MDA-MB-468 cells were infected with lentiviruses to establish MDA-MB-231-ICOSL, MDA-MB-468-ICOSL, MDA-MB-231-ICOSL-sg cell lines. Positive clones were selected with 1 µg/mL puromycin 48 hours post-transduction.

Immunoblotting

For the analysis of CAR-T cell expression efficiency, western blot analysis was performed using monoclonal mouse anti-FLAG (DYKDDDDK tag) antibody (1:5000, Cat No. 66008–4-Ig, Proteintech, Wuhan, Hubei, China), polyclonal rabbit anti-GAPDH antibody (1:5000, Cat No. 10494–1-AP, Proteintech), IRDye 800CW Goat anti-Rabbit secondary antibody (1:5000, Cat No. 926–32211, LI-COR, Lincoln, Nebraska, USA), and IRDye 680RD Goat anti-Mouse secondary antibody (1:5000, Cat No. 92668070, LI-COR). Membranes were visualized using the Odyssey CLX Imager (LI-COR Biosciences, USA) and analyzed with Image Studio Lite V.4.0 (LI-COR Biosciences, USA).

Flow cytometric analysis

For cell phenotype analysis, cells were stained in phosphate-buffered saline (PBS) with 0.5% bovine serum albumin using 5 µL of antibody per million cells in a 100 µL staining volume. Antibodies included mouse anti-human PE-ICOSL (Cat No. 13-5889-82, Thermo Fisher Scientific), PE-CD276 (B7H3) (Cat No. 351004, BioLegend) for tumor cell surface antigens, and PE-CD19 (Cat No. 302207, BioLegend), BB700-ICOS (Cat No. 46-9948-42, Thermo Fisher Scientific) for CAR and ICOS expression on T cells. Infiltration of T cells in tumor tissues in xenograft models was assessed using BB700-7AAD (Cat No. 420403, BioLegend), and BV510-CD8 (Cat No. 563919, BD Biosciences). Analysis was performed using Fluorescence Activated Cell Sorter (FACS, BD Biosciences) and FlowJo software (Tree Star, Ashland, North Carolina, USA).

Cell proliferation assay

Effector cells and target cells were co-cultured at a 1:3 ratio, with a control well-lacking target cells set concurrently. CAR-T cells were collected after 96 hours, and Ki-67 expression was evaluated using FACS to assess T cell proliferation. After extracellular staining, CAR-T cells were fixed and permeabilized with Cytofix/Cytoperm kit (Cat No. 554714, BD Biosciences) as per the manufacturer's instructions, followed by intracellular staining with anti-human PE-Ki-67 antibody (Cat No. 350503, BioLegend). Flow cytometric analysis was conducted, and data were analyzed using FlowJo software.

Cytotoxicity assay

MDA-MB-231 and MDA-MB-468 cells were infected with recombinant lentiviruses carrying the luciferase gene. After 48 hours, positive clones were selected using 200 µg/mL hygromycin. Luminescence levels were then measured with a microplate reader.[30] CAR-T cells were co-cultured with indicated cells at specified ratios in 96-well flat plates (Corning, Shanghai, China). Target cells alone were plated at the same density to determine maximal luciferase expression (relative light units, RLU).

After 24 hours of co-culture, luciferin (1.5 mg/mL, 100 µL per well; Cat No. 122799, PerkinElmer) was added, and luminescence was measured using a plate reader. Per cent lysis was calculated using the formula: $(1 - RLU_{sample}/RLU_{max}) \times 100\%$.

Xenogenic mouse models

To establish a humanized mouse model, 6-week-old female NSG mice (NOD.Cg-*Prkdc*^{scid}*IL2rg*^{em1Smoc}) were obtained from Shanghai Model Organisms (Shanghai, China) and housed in a specific pathogen-free animal facility. All animal procedures were approved by the Ethics Committee of Guangdong Provincial People's Hospital. NSG mice were subcutaneously inoculated with 5×10^6 MDA-MB-231 cells in 100 µL PBS into the left flank.[31] After 7 days, subcutaneous tumors became macroscopically visible, and 2.5×10^6 modified CAR-T cells were administered intravenously to the tumor-bearing mice. Recombinant hIL-2 (Cat No. BT-002–050, R&D Systems, Minneapolis, Minnesota, USA) was administered intraperitoneally at 1 µg per mouse every 3 days. Mice were monitored every 3 days for health status, tumor size was measured with calipers, and body weight was recorded. Mice were euthanized by carbon dioxide narcosis and cervical dislocation if weakness or tumor burden exceeded>1500 mm^3. For the metastasis model, 1×10^6 MDA-MB-231-Luc cells were injected via the tail vein of NSG mice, and lung metastasis foci were monitored using bioluminescence imaging.[32] After 14 days, metastatic lung tumors were established (with a total flux of approximately 1×10^7 p/s), and 5×10^6 modified CAR-T cells were intravenously administered to the tumor-bearing mice.

Enzyme-linked immunosorbent assay

CAR-T cells (10^5 cells) were co-cultured with target cells at a 3:1 ratio. After 24 hours, supernatants were collected for cytokine analysis using IFN-γ and TNF-α ELISA kits (Dakewe, China) according to the manufacturer's instructions. Cytokine levels in mouse serum were measured using a human IFN-γ and TNF-α ELISA Kit.

Immunohistochemistry

Paraffin-embedded breast cancer tissue microarrays were obtained from the National Engineering Center for Biochip (Outdo Biotech, Shanghai, China) with approval from the Outdo Biotech Clinical Research Ethics Committee. A cohort comprizing 33 cases of Luminal A, 16 cases of Luminal B, 43 cases of HER2$^+$, and 26 cases of TNBC was evaluated, with relevant clinical data provided in online supplemental table 1. Tissue sections were processed and stained following standard protocols by Biopathology Institute (Servicebio, Wuhan, Hubei, China). For antigen assessment, staining intensity was scored based on established criteria.[33] For antigen staining assessment, the intensity was scored as follows:[33] negative (0), weak (1), moderate (2), and strong (3). The extent of staining was graded based on the percentage of positively stained cells: 0 (<10%), 1 (10–25%), 2 (25–50%), 3 (50–75%), and 4 (>75%). In xenograft mouse models, euthanized mice were examined for organ health, including the heart, liver, spleen, lung, kidney, stomach, small intestine, large intestine, and pancreas. Organs were fixed in 4% formalin, paraffin-embedded, and subjected to H&E staining by Biopathology Institute (Servicebio). Images of H&E-stained sections were captured using a DM6B microscope (Leica, Wetzlar, Hessen, Germany).

Statistical analysis

Experiments were independently conducted at least three times. Data were analyzed using GraphPad Prism V.7.0 software (GraphPad Software, San Diego, California, USA) and presented as mean±SD. Statistical comparisons between two independent groups were performed using a two-tailed Student's t-test, while a one-way analysis of variance with Tukey's multiple comparisons test was used for multiple groups. Kaplan-Meier curves were used for the survival analysis of mice. Statistical significance was considered at $p<0.05$.

RESULTS

Aberrant ICOSL expression contributes to poor prognosis in patients with TNBC

ICOSL expression is predominantly found in professional antigen-presenting cells such as B cells, macrophages, and DCs.[15 34] ICOSL primarily modulates the function of T cells by binding to its receptor ICOS.[35] It has also been observed in specific endothelial cells and lung epithelium, as well as tumor cells such as melanoma and rhabdomyosarcoma, where it is associated with a poor prognosis in malignant carcinomas.[15 16] Whether ICOSL is expressed in breast cancer cells requires further examination. In an attempt to assess the clinical significance of ICOSL in breast cancer, we analyzed the messenger RNA expression of ICOSL in breast cancer tissue from the Cancer Genome Atlas (TCGA). ICOSL expression was particularly higher in basal-like breast cancer compared with HER2$^+$ and luminal$^+$ breast cancer tissues (figure 1A). Furthermore, Kaplan-Meier survival analysis showed that high expression of ICOSL especially correlated with shorter overall survival (OS) and poorer distant metastasis-free survival (DMFS) in patients with basal-like tumors but not HER2$^+$ and Luminal$^+$ breast cancer (figure 1B and online supplemental figure 1). Moreover, the protein levels of ICOSL were examined in 118 cases of breast cancer specimens compared with 40 cases of paratumor tissues, including a total of 33 cases of Luminal A, 16 cases of Luminal B, 43 cases of HER2$^+$, and 26 cases of TNBC (Online supplemental table 1). Immunohistochemistry (IHC) revealed that ICOSL was significantly overexpressed in TNBC compared with normal breast tissues (figure 1C). For assessing the expression levels of B7H3 and ICOSL in TNBC cell lines, flow cytometry analysis was performed. The frequency of B7H3 protein expression on TNBC cells exceeded 90%, ranging from 93.5% to 99.5%, whereas the frequency of ICOSL protein expression on TNBC

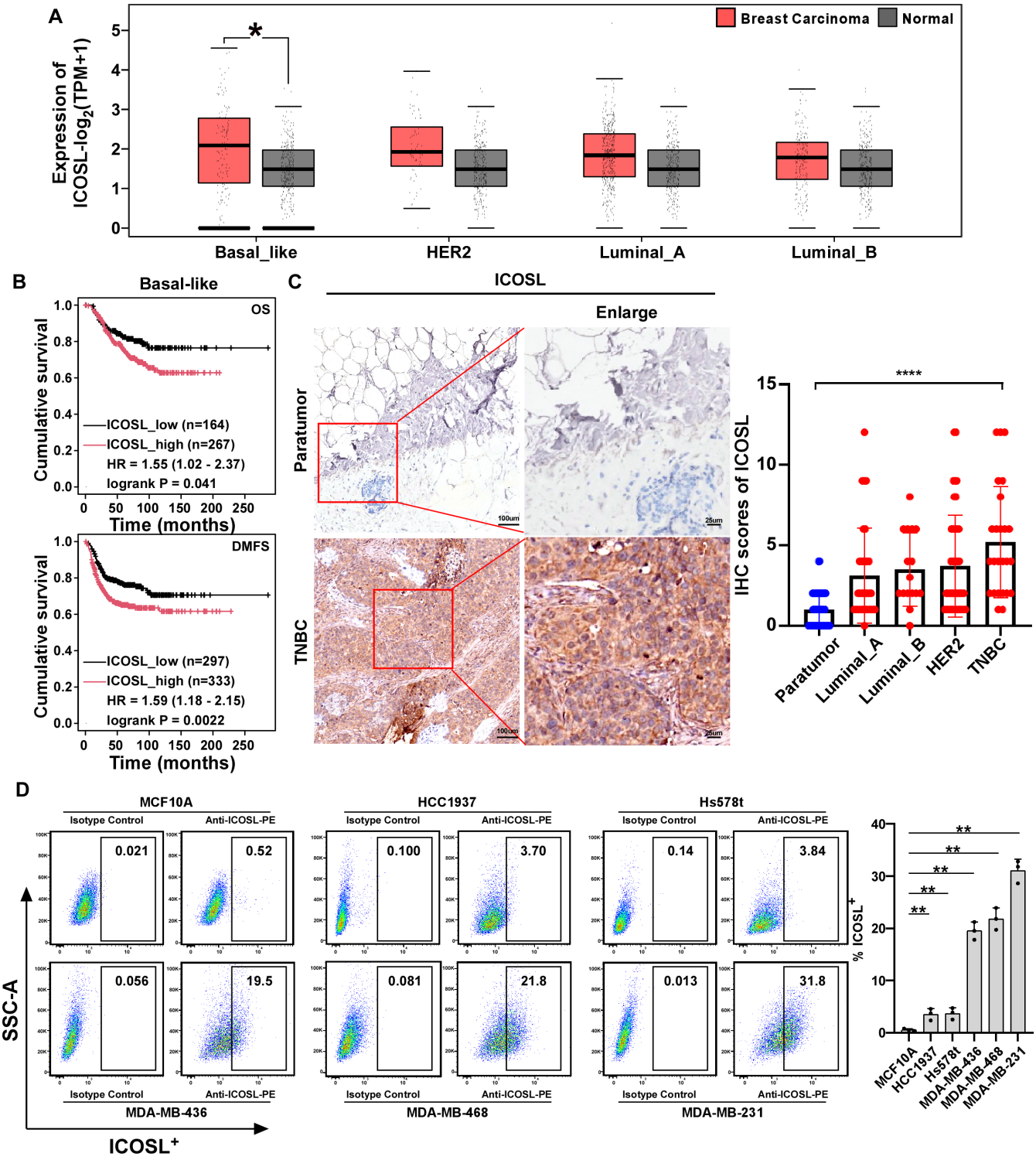

Figure 1 Elevated expression of ICOSL is associated with the development and poor outcome of TNBC. (A) Dysregulated expression of ICOSL in breast cancer from the TCGA cohort was analyzed using the GEPIA online service (http://gepia.cancer-pku.cn/). Patients were classified based on the intrinsic molecular subtypes of breast cancer. (B) Kaplan-Meier survival analysis was conducted to assess overall survival (OS) and distant metastasis-free survival (DMFS) according to the mRNA levels of ICOSL in the basal-like breast cancer, using the KM-plotter breast cancer database (http://kmplot.com/analysis/). (C) Representative images of ICOSL expression in TNBC and adjacent non-cancerous tissue (left panel). Quantitative IHC analysis of ICOSL (right panel). (D) Flow cytometry analysis was employed to evaluate the frequency of ICOSL protein levels on normal breast cell line and TNBC cell lines. Isotype antibody was used as a negative control. The statistical analysis was estimated by one-way ANOVA with Tukey's multiple comparisons test. Data are presented as mean values±SD. *p<0.05; **p<0.01; ****p<0.0001. ANOVA, analysis of variance; GEPIA, Gene Expression Profiling Interactive Analysis; HER2, human epidermal growth factor receptor 2; ICOSL, inducible costimulator ligand; IHC, immunohistochemistry; KM, Kaplan-Meier; mRNA, messenger RNA; TCGA, The Cancer Genome Atlas; TNBC, triple-negative breast cancer.

cells ranged from 3.70% to 31.8% (figure 1D and online supplemental figure 2). These expression levels were notably higher compared with the normal breast cell line, MCF10A (figure 1D and online supplemental figure 2). Collectively, these findings indicate that elevated levels of ICOSL contribute to poor prognosis in TNBC and may serve as a potential target for TNBC therapy.

Generation of ICOS-B7H3-CAR-T cells for immunotherapy

ICOS, a member of the CTLA4/CD28 family, plays a crucial role in regulating immune responses and T-cell differentiation.[17] Here, the scFv sequence of anti-human B7H3 was synthesized and fused to a third-generation CAR moiety. The B7H3-CAR was constructed using a lentiviral vector, and the ICOS-B7H3-CAR was subsequently designed based on it, incorporating the overexpression of ICOS (figure 2A). Flow cytometry analysis revealed that the lentiviral transduction efficiency of CAR-T cells exceeded 40% (figure 2B and online supplemental figure 3A). Moreover, western blot analysis demonstrated the efficient expression of CAR-T cells (figure 2C). Additionally, the expression of ICOS on ICOS-B7H3-CAR-T cells was 51.6%, which was higher compared with control T cells (figure 2D and online supplemental figure 3B). To further assess the function of B7H3-CAR-T and ICOS-B7H3-CAR-T cells, a cytotoxicity assay was conducted by co-culturing CAR-T cells with TNBC cell lines. MDA-MB-231 and MDA-MB-468 cells were obtained and transduced with firefly luciferase lentivirus. B7H3-CAR-T cells exhibited dose-dependent and specific cytotoxicity against TNBC cells, with approximately 40% cytotoxic effect at an effector-to-target ratio of 3:1, while ICOS-B7H3-CAR-T cells demonstrated even greater cytotoxicity, with over 60% cytotoxic effect (figure 2E–2F). Consistently, ICOS-B7H3-CAR-T cells upregulated the secretion of IFN-γ and TNF-α compared with B7H3-CAR-T cells (figure 2G–2J). Taken together, these data suggested that ICOS-expressing CAR-T cells enhanced cytotoxicity against TNBC cells to a greater extent by secreting TNF-α and IFN-γ.

ICOS-B7H3-CAR-T cells exhibit superior antitumor activity in vivo

To further confirm the antitumor activity of ICOS-B7H3-CAR-T cells in vivo, a xenograft tumor model was assessed. MDA-MB-231 tumor cells were implanted subcutaneously in NSG mice. After tumor formation on day 7, ICOS-B7H3-CAR-T cells and control CAR-T cells were administered separately to the mice via a single intravenous injection (figure 3A). As depicted in figure 3B, therapy using ICOS-B7H3-CAR-T cells resulted in decreased TNBC tumor size compared with B7H3-CAR-T therapy. Consistently, both tumor volume and weight were significantly reduced following treatment with ICOS-B7H3-CAR-T cells (figure 3C–3D). Subcutaneous tumors from mice were subjected to H&E staining, revealing that the tumor tissue of mice treated with ICOS-B7H3-CAR-T exhibited more pronounced necrosis (figure 3E). Importantly, the infiltration of ICOS-B7H3-CAR-T cells was notably enhanced in the xenograft tumor tissue compared with B7H3-CAR-T cells based on immunostaining for CD8 (figure 3F and online supplemental figure 4). Furthermore, ICOS-B7H3-CAR-T cell therapy significantly increased the levels of effector cytokines in mouse serum, including TNF-α and IFN-γ (figure 3G–3H). A safety evaluation of adoptive CAR-T cells in vivo was conducted, including monitoring mouse weight and assessing major tissue organs. As depicted in online supplemental figure 5, mouse weight and the function of major organs remained normal during adoptive CAR-T therapy, indicating the safety of modified CAR-T cells. Thus, ICOS enhanced the antitumor activity of B7H3-CAR-T cells, suggesting its potential as a marker to enhance the cytotoxicity of CAR-T therapy.

ICOS-B7H3-CAR-T cells have prolonged antitumor activity in vivo and could eradicate metastasis

To further assess whether ICOS extends the antitumor activity of B7H3-CAR-T cells in vivo and eradicates metastasis of TNBC, NSG mice were intravenously injected with Luc-transduced MDA-MB-231 cells via the tail vein. Two weeks later, ICOS-B7H3-CAR-T, B7H3-CAR-T, and GP120-CAR-T cells were administered via a single intravenous injection (figure 4A). Clearly, ICOS-B7H3-CAR-T cell therapy significantly prolonged overall survival compared with B7H3-CAR-T cell therapy (figure 4B). Additionally, ICOS-B7H3-CAR-T cells effectively eliminated metastasis of TNBC without tumor recurrence (figure 4C–4D). In contrast, B7H3-CAR-T cells failed to eliminate TNBC metastasis, and the tumor burden worsened (figure 4C–4D). At the humane endpoint, the mice were euthanized, and metastatic lesions were assessed using bioluminescence imaging (figure 4E). Among the three groups, the ICOS-B7H3-CAR-T cell treatment group demonstrated the most effective eradication of TNBC metastasis compared with both the B7H3-CAR-T and GP120-CAR-T cell groups (figure 4E). Additionally, the infiltration of ICOS-B7H3-CAR-T cells into the xenograft tumor tissue was significantly enhanced compared with B7H3-CAR-T cells based on immunostaining for CD8 (figure 4F and online supplemental figure 6). Furthermore, ICOS-B7H3-CAR-T cell therapy markedly increased the levels of effector cytokines in mouse serum, including TNF-α and IFN-γ (figure 4G). Overall, these data demonstrated that ICOS enhanced the in vivo cytotoxicity of CAR-T cells and contributed to the durable eradication of metastasis tumor.

ICOSL expression on tumor cells enhances the antitumor activity of ICOS-B7H3-CAR-T cells

Based on the results observed above, ICOSL was found to be highly expressed in TNBC tissue and correlated with a poor prognosis for patients with TNBC. As a ligand of ICOS, ICOSL enhances the function of effector T cells by binding to ICOS.[17] Considering the expression of ICOS, ICOS-B7H3-CAR-T cells exhibit superior antitumor activity in vitro and in vivo. To further explore whether the cytotoxicity of ICOS-B7H3-CAR-T cells is influenced by

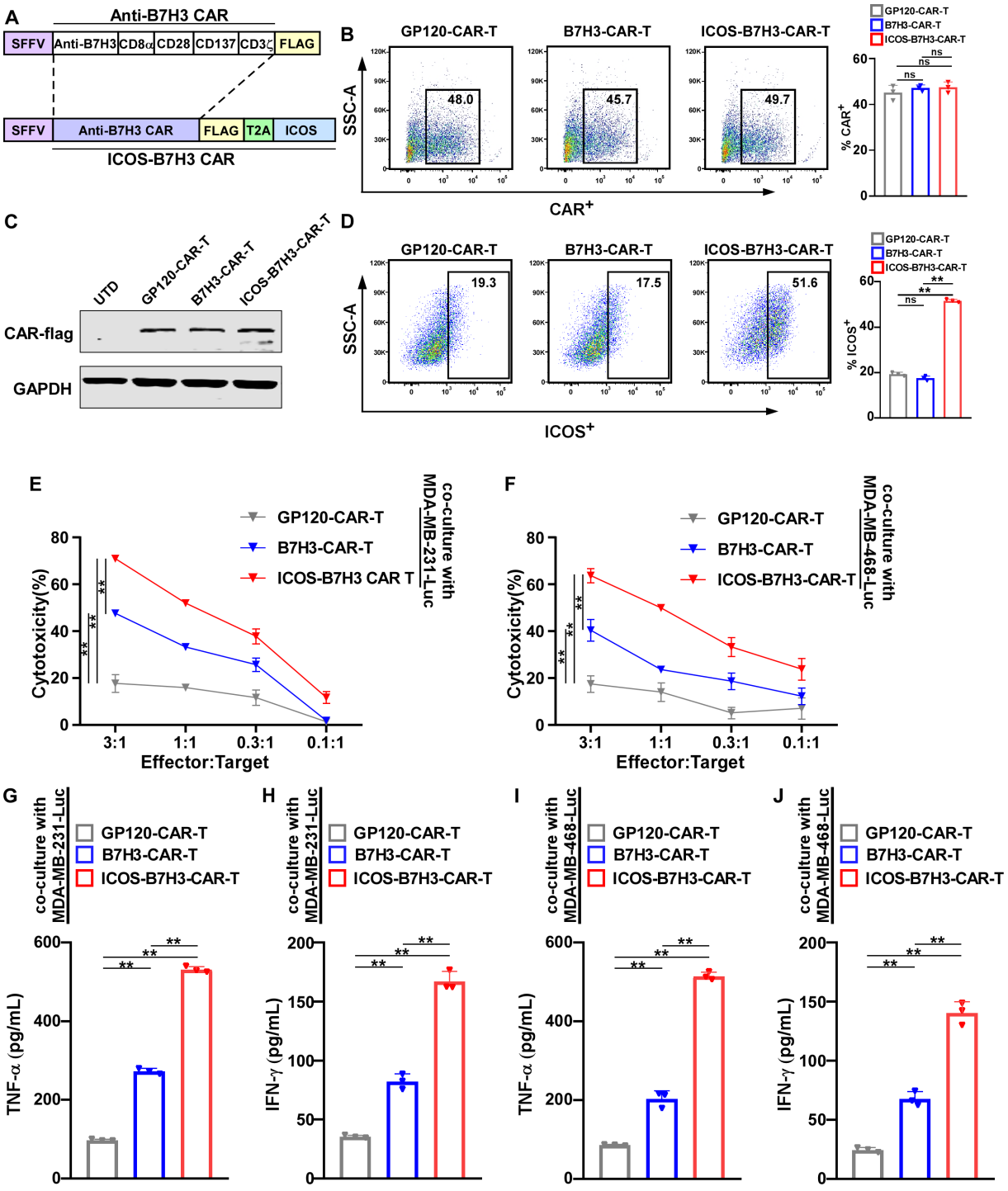

Figure 2 ICOS was incorporated into the construction of B7H3-CAR-T cells for cellular immunotherapy. (A) Schematic representation of the single-chain variable fragment (scFv) targeting human B7H3 fused with a third-generation CAR moiety using a lentiviral vector (B7H3-CAR), and ICOS-B7H3-CAR includes the overexpression of ICOS based on it. (B) Flow cytometry analysis was employed to evaluate the frequency of CAR protein expression levels on T cells among different groups. (C) Western blot analysis was conducted to assess the expression of B7H3-CAR and ICOS-B7H3-CAR using anti-flag antibody. GP120-CAR-T cells were used as mock CAR-T controls. Untransduced T cells served as the negative control. (D) Flow cytometry analysis was employed to evaluate the frequency of ICOS protein expression levels on T cells among different groups. (E–F) The cytotoxic activity of B7H3-CAR and ICOS-B7H3-CAR was assessed using a luciferase reporter system after 24 hours of co-culture with MDA-MB-231-Luc and MDA-MB-468-Luc cells at various effector-to-target (E:T) ratios. (n=3, 3 healthy donors). GP120-CAR-T cells as negative control. (G–J) The levels of effector cytokines (TNF-α and IFN-γ) in the supernatant of CAR-T cells were measured by ELISA after 24 hours of co-culture with tumor cells. The statistical analysis was estimated one-way ANOVA with Tukey's multiple comparisons test. Data are presented as mean values±SD. **p<0.01. ANOVA, analysis of variance; CAR, chimeric antigen receptor; ICOS, inducible costimulator; IFN-γ, interferon gamma; ns, not significant; TNF-α, tumor necrosis factor alpha.

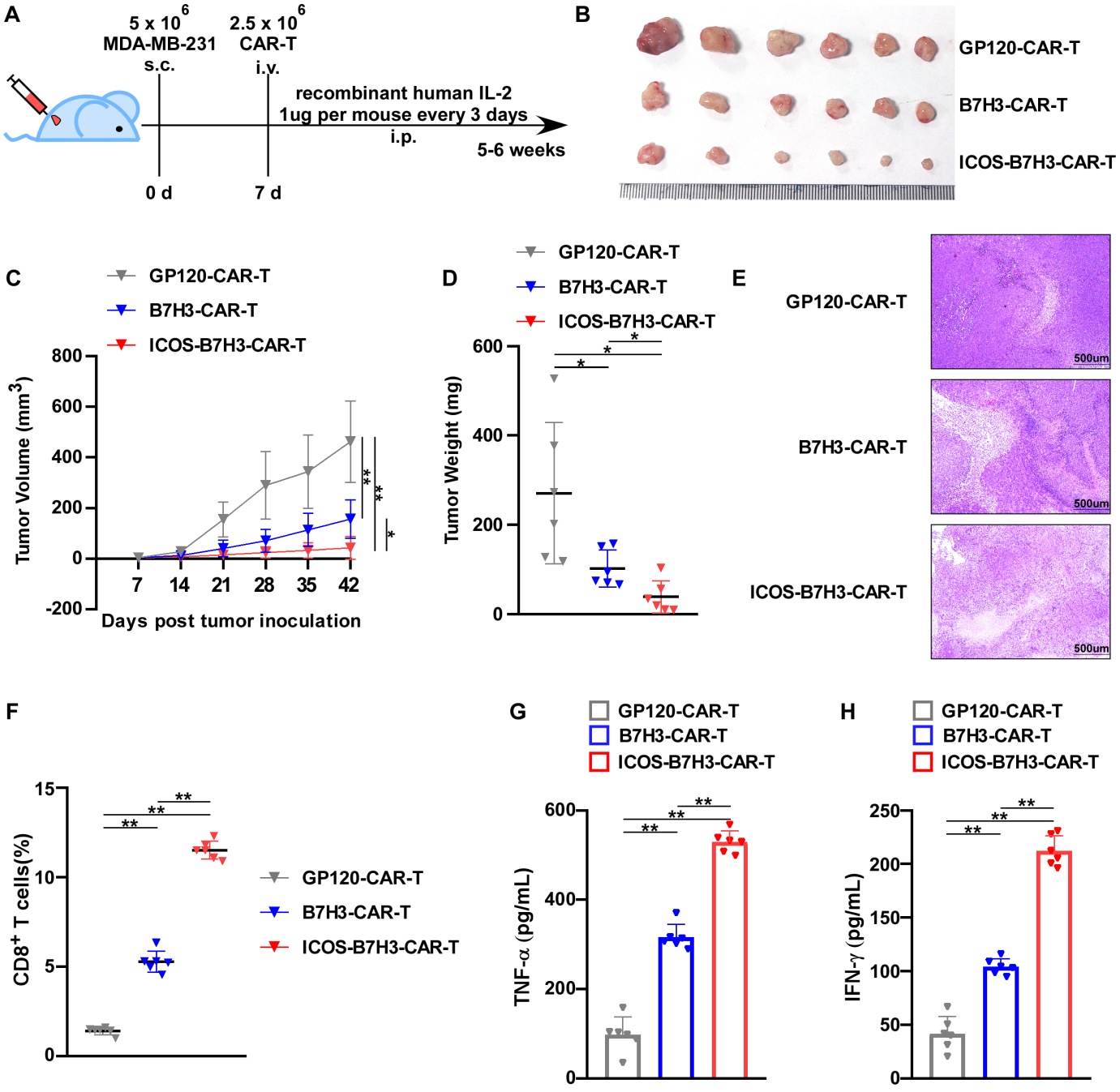

Figure 3 ICOS-B7H3-CAR-T cells exhibited superior antitumor activity in vivo. (A) Schematic diagram of a xenograft model where MDA-MB-231 cells were inoculated subcutaneously into NSG mice, followed by infusion of various CAR-T cells via tail injection. (B) Representative images of mice bearing tumors after receiving different CAR-T treatments (n=6). (C–D) Tumor volumes and tumor weights were assessed in mice bearing tumors after receiving different CAR-T treatments (n=6). (E) The H&E staining of mouse tumors after CAR-T therapy. (F) The percentage of infiltrating CAR-T cells in mice bearing tumors after receiving different treatments (n=6). (G–H) The levels of effector cytokines (TNF-α and IFN-γ) in mouse serum homogenate were measured by ELISA (n=6). The statistical analysis was estimated one-way ANOVA with Tukey's multiple comparisons test. Data are presented as mean values±SD. *p<0.05; **p<0.01. ANOVA, analysis of variance; CAR, chimeric antigen receptor; ICOS, inducible costimulator; IFN-γ, interferon gamma; TNF-α, tumor necrosis factor alpha.

ICOSL expression on tumor cells, we examined the function of ICOSL in TNBC cells by transducing them with ICOSL overexpression and ICOSL-sg lentiviral vectors. MDA-MB-231 and MDA-MB-468 cells were transduced with an ICOSL overexpression lentiviral vector (online supplemental figure 7). Overexpression of ICOSL in tumor cells significantly enhanced the cytotoxic activity of ICOS-B7H3-CAR-T cells but did not affect the cytotoxic activity of B7H3-CAR-T cells (figure 5A–5B). Furthermore, when co-cultured with ICOSL-overexpressing tumor cells, effector cytokines including IFN-γ and TNF-α were upregulated in ICOS-B7H3-CAR-T cells, while the

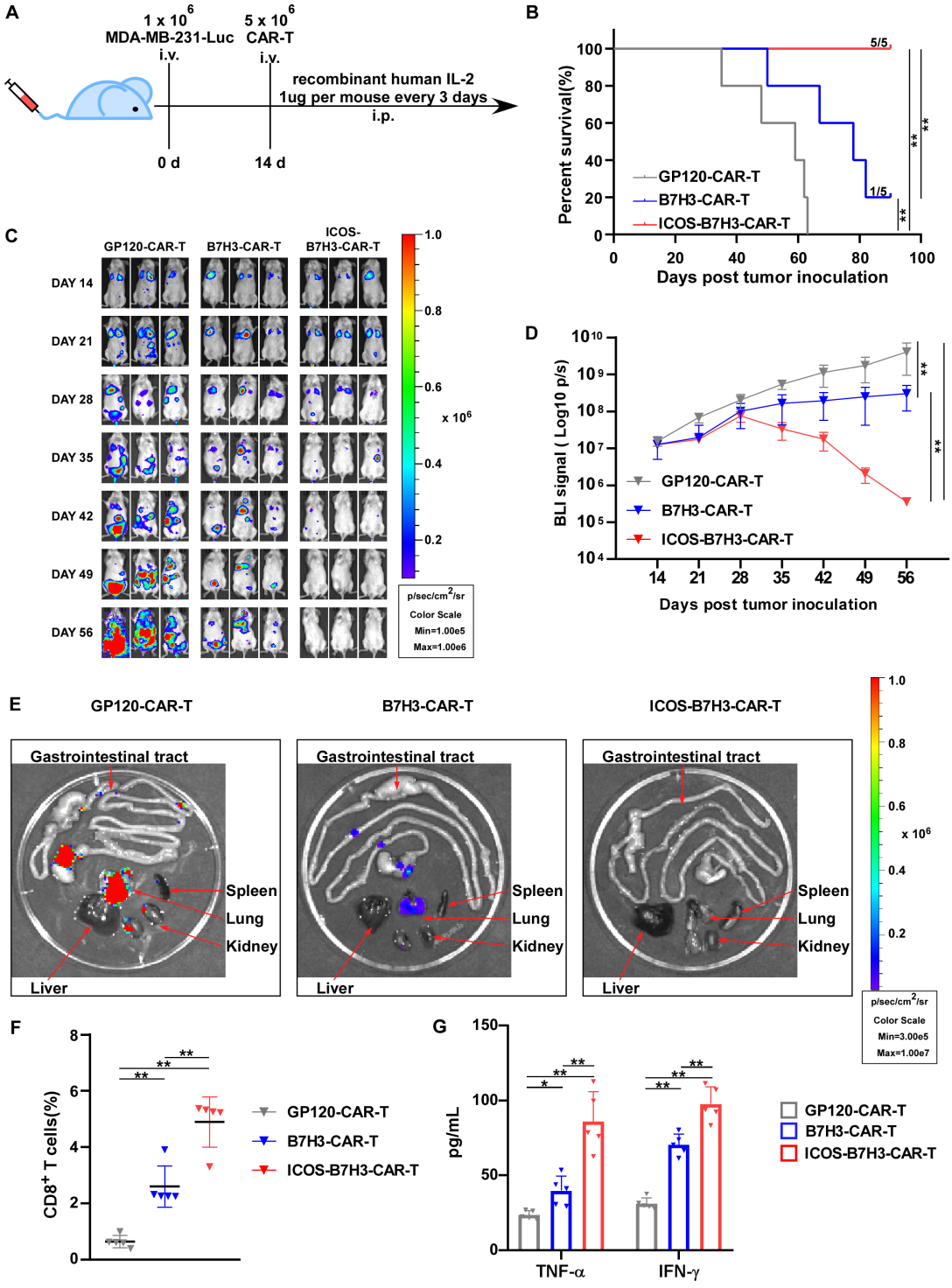

Figure 4 ICOS-B7H3-CAR-T cells have prolonged antitumor activity in vivo could eradicate metastasis. (A) Schematic diagram of a metastatic xenograft model involving the intravenous injection of MDA-MB-231 cells into NSG mice, followed by treatment with various CAR-T cells via tail injection 2 weeks later. (B) Kaplan-Meier survival analysis of mice under different CAR-T treatments. (n=5). (C) Representative bioluminescence (BLI) images depicting the growth of MDA-MB-231-Luc tumors in the metastatic xenograft model under different CAR-T treatments. Tumor progression was monitored using an in vivo imaging system (IVIS) every 7 days. (D) BLI kinetics illustrating the growth of MDA-MB-231-Luc tumors in the metastatic xenograft model under different CAR-T treatments. (n=5). (E) Representative BLI images of metastatic lesions in the xenograft model under different CAR-T treatments. Red arrows indicate major organs. (F) The percentage of infiltrating CAR-T cells in tumors from the metastatic xenograft model after receiving different treatments. (n=5). (G) The levels of effector cytokines (TNF-α and IFN-γ) in mouse serum homogenate were measured by ELISA (n=5). The statistical analysis was estimated one-way ANOVA with Tukey's multiple comparisons test. Data are presented as mean values±SD. *p<0.05; **p<0.01; ***p<0.001. ANOVA, analysis of variance; CAR, chimeric antigen receptor; ICOS, inducible costimulator; IFN-γ, interferon gamma; ip, intraperitoneal; iv, intravenous; TNF-α, tumor necrosis factor alpha.

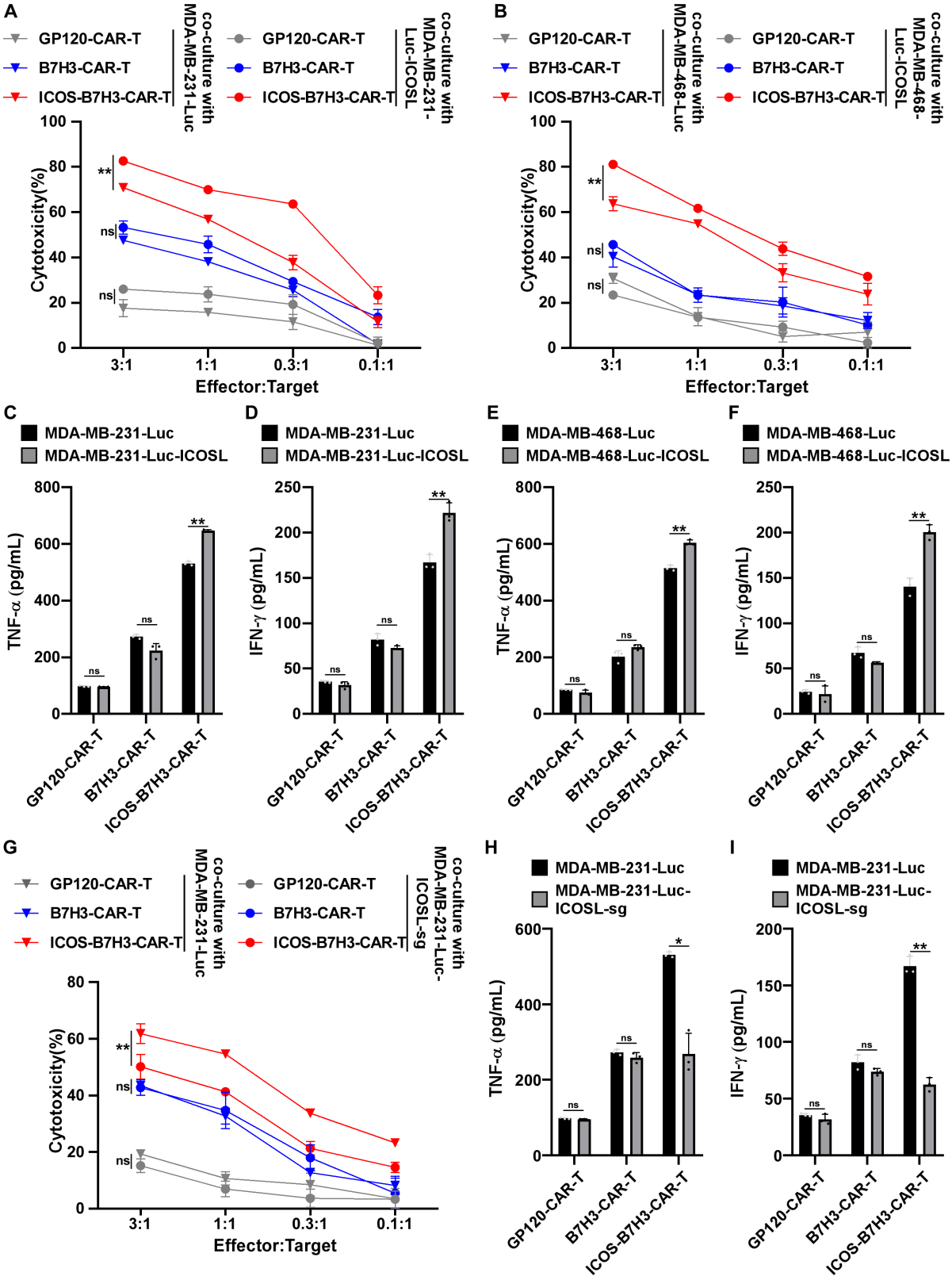

Figure 5 The overexpression of ICOSL in TNBC cells enhanced the cytotoxic function of ICOS-B7H3-CAR-T cells, while knocking out ICOSL expression diminishes it. (A–B, G) The cytotoxic activity of B7H3-CAR and ICOS-B7H3-CAR was assessed using a luciferase reporter system after 24 hours of co-culture with indicated TNBC cells at various effector-to-target (E:T) ratios. (n=3, 3 healthy donors). GP120-CAR-T cells as negative control. (C–F, H–I) The levels of effector cytokines (TNF-α and IFN-γ) in the supernatant of CAR-T cells were measured by ELISA after 24 hours of co-culture with tumor cells. The statistical analysis was estimated by two-tailed Student's t-test. Data are presented as mean values±SD. *p<0.05; **p<0.01. CAR, chimeric antigen receptor; ICOSL, inducible costimulator ligand; IFN-γ, interferon gamma; ns, not significant; TNBC, triple-negative breast cancer; TNF-α, tumor necrosis factor alpha.

expression of ICOSL did not affect the levels of TNF-α and IFN-γ in B7H3-CAR-T cells (figure 5C–5F), indicating that the increased expression of ICOSL on tumor cells was essential for the cytotoxicity of ICOS-B7H3-CAR-T cells. Additionally, sgRNA-guided CRISPR-Cas9 targeting ICOSL was employed to KO the endogenous expression of ICOSL in MDA-MB-231 cells (online supplemental figure 7). Consistently, knocking out the expression of ICOSL in MDA-MB-231 cells restored the cytotoxicity and secretion levels of TNF-α and IFN-γ of ICOS-B7H3-CAR-T cells, bringing them down to the levels observed in B7H3-CAR-T cells (figure 5G–5I). Compared with control T cells, ICOS had no effect on the proliferation of T cells based on CAR expression (figure 6 and online

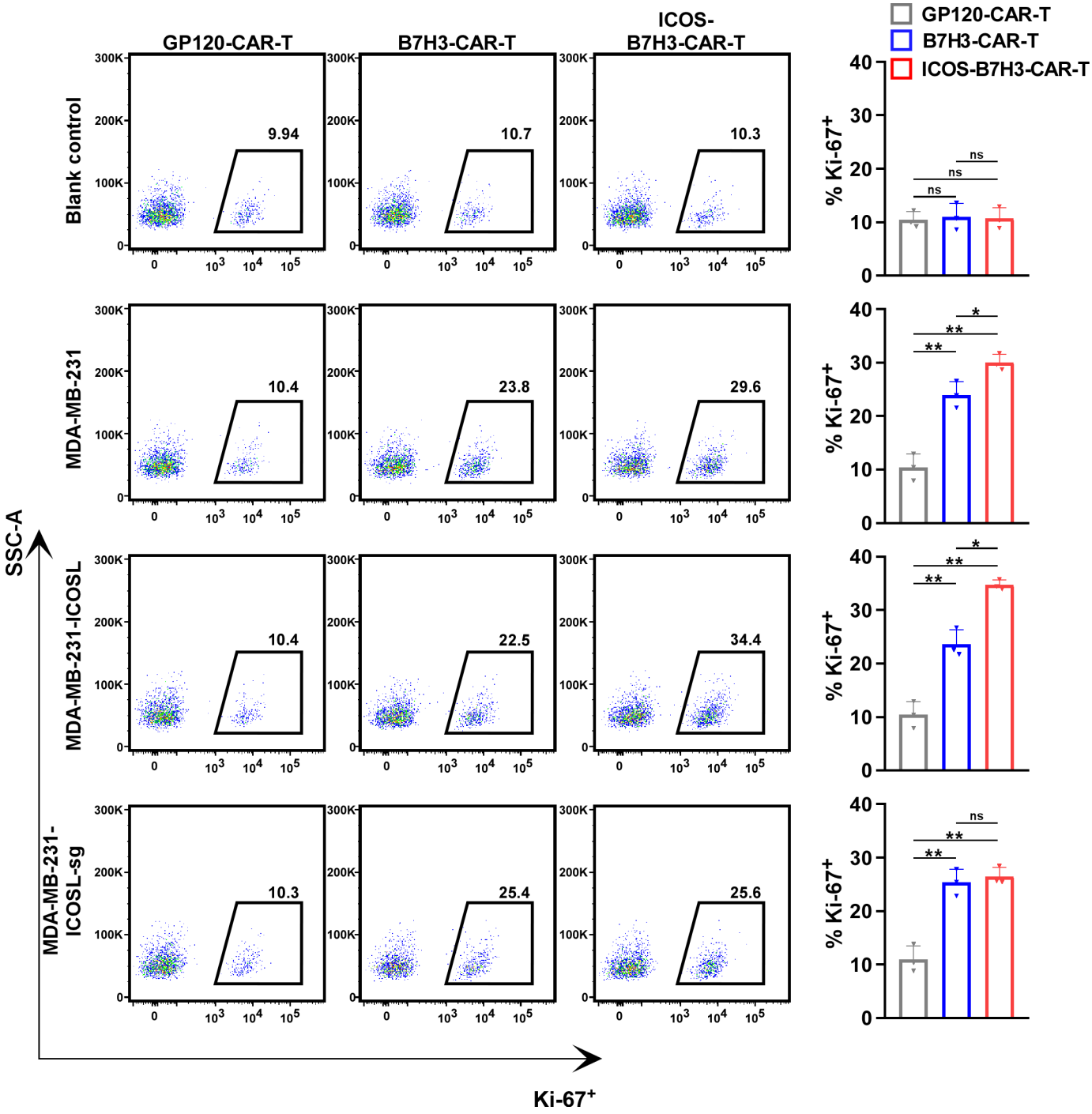

Figure 6 The proliferative capacity of CAR-T cells was assessed on co-culture with tumor cells. Flow cytometry was employed to measure the intensity of Ki-67, indicating the proliferation of CAR-T cells, following co-incubation with specific tumor cells (left panel). Quantitative analysis was performed to evaluate the proliferation of CAR-T cells (right panel). The statistical analysis was estimated one-way ANOVA with Tukey's multiple comparisons test. Data are presented as mean values±SD. *p<0.05; **p<0.01. ANOVA, analysis of variance; CAR, chimeric antigen receptor; ICOSL, inducible costimulator ligand; ns, not significant.

supplemental figure 8). However, when co-cultured with tumor cells, the proliferation of B7H3-CAR-T cells was significantly higher than that of control T cells, while ICOS-B7H3-CAR-T cells exhibited even greater proliferation (figure 6). Furthermore, the expression of ICOSL in tumor cells significantly enhanced the proliferation of ICOS-B7H3-CAR-T cells. Conversely, knocking out the expression of ICOSL in MDA-MB-231 cells restored the proliferation of ICOS-B7H3-CAR-T cells to levels observed in B7H3-CAR-T cells (figure 6). Therefore, these data suggest that the level of ICOSL on the tumor enhances the cytotoxic capability and proliferation efficiency of ICOS-B7H3-CAR-T cells, as well as their potency of TNF-α and IFN-γ secretion.

In conclusion, we engineered $CD8^+$ CAR-T cells with elevated ICOS expression targeting the B7H3 antigen, and found that it bolstered their antitumor efficacy. The effect is amplified when it is co-cultured with breast cancer cell types that exhibit high levels of ICOSL. In comparison to standard B7H3-CAR-T cells, our ICOS-B7H3-CAR-T cells displayed sustained antitumor activity, effectively eradicating metastases both in vitro and in vivo, accompanied by increased secretion of cytokines such as IFN-γ and TNF-α (figure 7). Notably, manipulating ICOSL expression levels on TNBC cells, either by overexpression or KO, had a profound influence on the functionality of ICOS-B7H3-CAR-T cells, emphasizing the critical role of ICOSL expression in TNBC cells for the superior antitumor effects of ICOS-B7H3-CAR-T cells.

DISCUSSION

Accumulating evidence shows that ICOS plays a pivotal role in the function of effector T cells, garnering a lot of attention as a potential target for immunotherapy. Of significant relevance, the percentage of $ICOS^{hi}CD4^+$ cells increased in the peripheral blood and tumor tissues of patients with cancer following treatment with anti-CTLA-4 mAbs, which led to increased production of IFN-γ and an elevated ratio of effector to Tregs.[36–38] IVAX, a cellular vaccine expressing ICOSL, triggers ICOS expression on CD8 and CD4 Teff cells, resulting in a dramatic

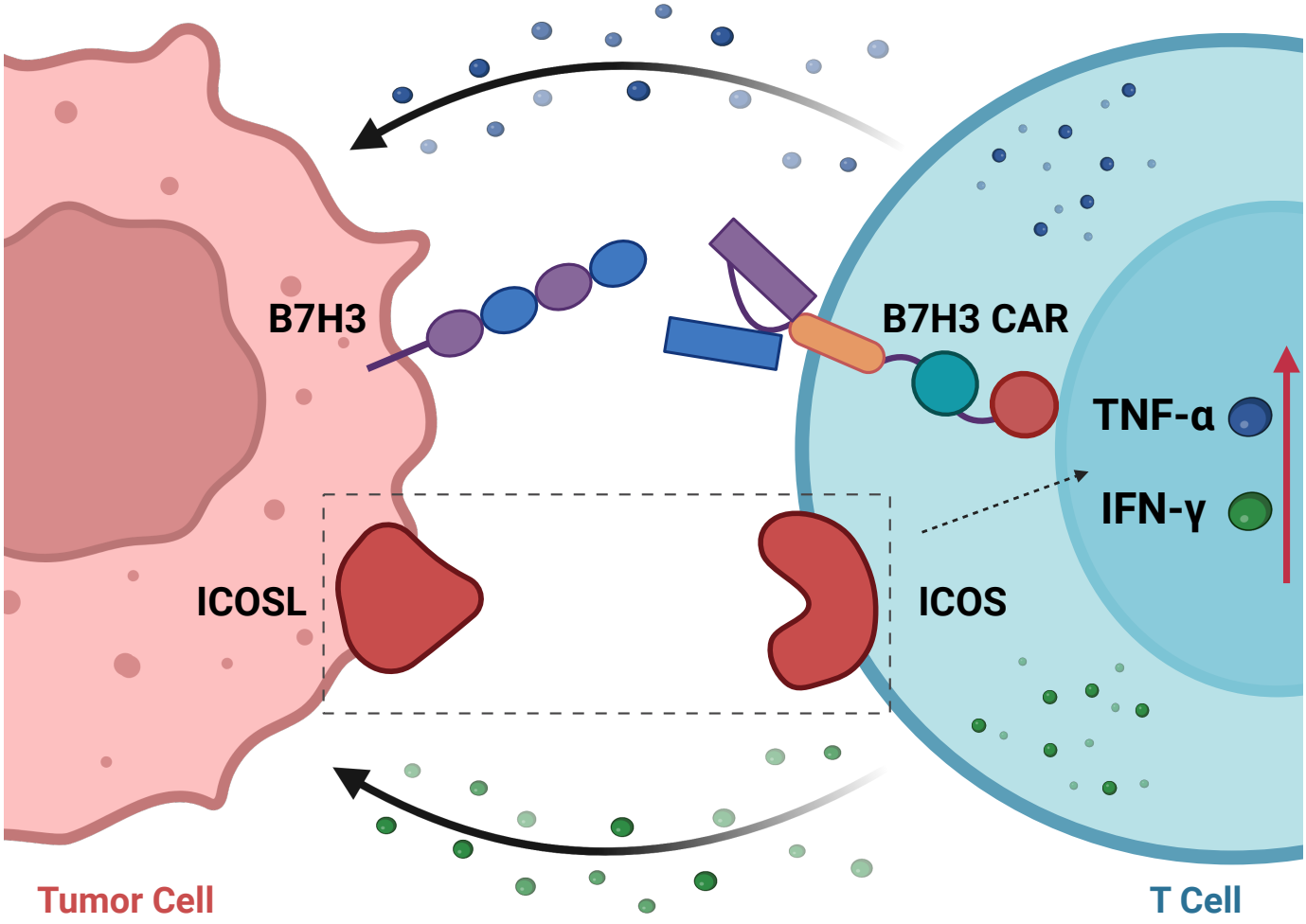

Figure 7 Schematic depiction of the function of ICOS-B7H3-CAR-T cells targeting TNBC cells expressing both B7H3 and ICOSL. CAR, chimeric antigen receptor; ICOSL, inducible costimulator ligand; IFN-γ, interferon gamma; TNBC, triple-negative breast cancer; TNF-α, tumor necrosis factor alpha.

enhancement of tumor rejection that synergizes with CTLA-4 blockade.[38] However, only IVAX treatment fails to eradicate the tumor, suggesting that ICOS might play an important role in the therapeutic effect of ICB.[38] The combination of the anti-ICOS agonist feladilimab with the anti-CTLA-4 antibody tremelimumab was evaluated in a phase I/II trial for the treatment of patients with select advanced solid tumors (NCT03693612).[39] However, the efficacy of the clinical trial is limited. All patients experienced at least one adverse event, and only one patient achieved a partial response (3.8%),[39] highlighting the need for further exploration of ICOS's role in cancer therapy. Accumulating evidences have determined that ICOS/ICOSL signaling plays various roles in cancers, depending on the specific cell type involved.[15 34] Hence, more therapeutic strategies targeting ICOS/ICOSL are in urgent need to be developed.

Within the spectrum of breast cancers, TNBC stands out as the most aggressive subtype and often associated with a grim prognosis.[2] TNBC often presents with frequent recurrence and metastasis, yet conventional treatments frequently result in drug resistance.[2] CAR-T therapy has shown promising antitumor efficacy in the treatment of TNBC.[5–7] However, the effectiveness of CAR-T therapy against solid tumors in patients has been considerably constrained. This restriction primarily arises from factors including the limited specificity and extensive heterogeneity of tumor antigens, insufficient T-cell penetration into tumors, and the immunosuppressive tumor microenvironment, which can trigger T-cell exhaustion and impairment.[12 40] In our study, analysis of breast cancer samples from the TCGA database revealed higher ICOSL expression in basal-like breast cancer, correlating with shorter OS and poorer DMFS in patients with this subtype. IHC and flow cytometry showed that ICOSL was highly expressed in breast cancer tissues and cell lines. Therefore, the construction of CAR-T cells targeting ICOSL on TNBC cells might exert antitumor efficacy.

ICOSL primarily modulates the function of T cells by binding to its receptor ICOS.[35] Multiple evidences show that ICOS facilitates the expansion and functionality of various T helper subsets (including TH1, TH2, TH17, and TFH cell subsets) as well as Treg cells, with its effects being contingent on the specific context.[41 42] ICOS was proved to induce the expression of Bcl6, providing an early signal to induce TFH cell differentiation via CXCR5, which is helpful for GC formation and adaptive immune responses.[42] Interestingly, ICOS was also proved to affect the function and differentiation of $CD8^+$ T cells. For example, heightened ICOS expression serves as a distinctive feature of $CD8^+$ tissue-resident memory T cells, crucial for their migration to non-lymphoid tissues by interacting with ICOSL.[43] Moreover, $CD8^{CXCR5+\ ICOS+}$ cells share phenotypic features with TFH cells, secreting IL-4, IL-21, CXCL13 and possessing the capacity to support B cells.[44 45] CAR-T cells often use a combination of $CD4^+$ and $CD8^+$ T cells. Interestingly, $CD4^+$ CAR-T cells have demonstrated strong antitumor effects, occasionally outperforming $CD8^+$ CAR-T cells in specific preclinical tumor models.[46–48] However, $CD4^+$ CAR-T cells sometimes exhibit limited or decreased effectiveness compared with their $CD8^+$ counterparts.[49 50] The impact of ICOS/ICOSL signaling on cancer is complex and varies depending on the predominant cell type involved. ICOS-conducted signaling in $CD8^+$ T cells and certain subsets of $CD4^+$ T cells, such as Th1 and TFH cells, generally promotes antitumor activity.[51 52] In contrast, ICOS-conducted signaling in Tregs typically contributes to immunosuppressive effects.[38] These findings suggest that ICOS may play distinctive roles in $CD4^+$ and $CD8^+$ T cells, particularly in modulating the function of Tregs. Hence, we developed $CD8^+$ CAR-T cells (ICOS-B7H3-CAR), rather than $CD4^+$ CAR-T cells, based on third-generation CAR-T cell technology, which featured heightened ICOS expression and targeted the B7H3 antigen. ICOS-B7H3-CAR-T cells demonstrated enhanced antitumor activity compared with conventional B7H3-CAR-T cells, both in vitro and in vivo, by producing elevated levels of cytokines like IFN-γ and TNF-α. Notably, ICOS-B7H3-CAR-T cells exhibited increased infiltration into xenograft tumor tissue compared with B7H3-CAR-T cells. In our metastasis model, we observed multiple metastases in untreated MDA-MB-231 tumors in NSG mice. While B7H3-CAR-T cells could suppress tumor growth in early treatment, their persistence was limited, making it difficult to effectively control subsequent tumor growth. However, the introduction of ICOS extended the efficacy and persistence of CAR-T cells, enabling effective clearance of metastases and prolonged survival. To further explore the underlying mechanism of the ICOS molecule, we overexpressed and knocked out the expression of ICOSL in TNBC cells. When co-cultured with ICOSL-overexpressed TNBC cells, ICOS-B7H3-CAR-T cells demonstrated potent superior cytotoxicity and proliferation efficiency, while its KO restored cytotoxicity, cytokine secretion and proliferation efficiency to levels seen in B7H3-CAR-T cells. This underscores the importance of ICOSL expression levels on TNBC cells for the superior antitumor effects of ICOS-B7H3-CAR-T cells.

Activation of the ICOS receptor increases PIP3 production, leading to Akt activation, which supports cellular proliferation and survival.[53 54] The unique YMFM motif, in the cytoplasmic tail of ICOS (as opposed to YMNM in CD28), is essential for the selective recruitment of the p50α subunit of PI3K, which exhibits higher lipid kinase activity than p85α has.[53] Several studies have demonstrated that the CAR-T cells harboring the TMD and/or ICD fragments of ICOS exhibited better efficiency in immunotherapy.[23–25] The ICOS TMD promotes the association of the ICD of CAR-T moiety with tyrosine kinase Lck, leading to enhanced PI3K activation.[25] In our study, we developed a CAR-T cell by expressing a full length of ICOS on the surface of CAR-T cells. This modification improves CAR-T cell efficacy by enabling binding to ICOSL on tumor cells and simultaneously magnifying its superior antitumor cytotoxicity and lasting elimination of metastasis by ICOS-B7H3 CAR-T cells in TNBC.

Additionally, the impact of ICOS/ICOSL on cancer function varies depending on the dominant cell type involved, highlighting the need for further exploration. It will be intriguing to examine whether Tregs exhibit distinct properties when exposed to ICOS-B7H3 CAR-T cell treatment. Future research endeavors should focus on developing strategies that use the ICOS stimulation pathway to enhance the cytotoxicity and durable function of $CD8^+$ T cells, while minimizing the effects on Tregs, to achieve more effective induction of protective immunity in barrier tissues. Overall, our findings highlight the potential clinical utility of ICOS as a promising strategy for addressing TNBC recurrence and metastasis.

Author affiliations
[1]Medical Research Institute, Guangdong Provincial People's Hospital (Guangdong Academy of Medical Sciences), Southern Medical University, Guangzhou, Guangdong, China
[2]Department of Breast Surgery, the Second Affiliated Hospital, Guangzhou Medical University, Guangzhou, Guangdong, China
[3]Guangzhou National Laboratory, Guangzhou International Bio-Island, Guangzhou, Guangdong, China
[4]Department of Gynecology, Guangdong Provincial People's Hospital (Guangdong Academy of Medical Sciences), Southern Medical University, Guangzhou, Guangdong, China
[5]Guangdong Cardiovascular Institute, Guangdong Provincial People's Hospital (Guangdong Academy of Medical Sciences), Guangzhou, Guangdong, China
[6]Institute of Human Virology, Key Laboratory of Tropical Disease Control of Ministry of Education, Guangdong Engineering Research Center for Antimicrobial Agent and Immunotechnology, Zhongshan School of Medicine, Sun Yat-sen University, Guangzhou, Guangdong, China

Contributors LC, HP, YC and BX contributed equally to this work. FY, HY, HZ and XC are senior and corresponding authors who also contributed equally to this study. LC, HP, YC, BX, FY, HY, HZ and XC have full access to all the data in this study and take full responsibility as guarantors for the integrity of the data and the accuracy of the data analysis. LC, HP and YC designed experiments. HP, BX and TZ performed the bioinformatics analysis. HP, BX, TZ, JG and YC performed the experiments and analyzed and interpreted the data. LC, FY, HY, XC and HZ supported and supervised the research. LC and HP wrote the manuscript, and all authors read and approved the final manuscript. During the preparation of this work, the author used ChatGPT V.3.5 to assist with article polishing and grammar checking. After using this tool, the author reviewed and edited the content and takes full responsibility for the publication's content.

Funding This work was supported by the National Natural Science Foundation of China (grant numbers 82103534), Guangdong Basic and Applied Basic Research Foundation (grant numbers 2020A1515110994, 2021A1515011500) to LC. This work was supported by Talent Research Funding of Guangdong Provincial People's Hospital (grant number KJ012019376) to HZ. This work was supported by Guangzhou Basic Research Program Municipal School (Hospital) Joint Funded Foundation and Application Basic Research Project (202201020115) to XC. This work was also supported by the Guangdong Basic and Applied Basic Research Foundation (2022A1515010243) to HY. This work was also supported by the National Natural Science Foundation of China (82102367), and the Guangdong Basic and Applied Basic Research Foundation (2022A1515012422) to FY. We would like to express our gratitude to these funding sources for their support.

Competing interests No, there are no competing interests.

Patient consent for publication Not applicable.

Ethics approval In this study, blood samples were anonymized in accordance with local ethical guidelines and the Declaration of Helsinki. All procedures of this study were approved by the Ethics Committee for Clinical Research and Application of the Second Affiliated Hospital of Guangzhou Medical University. (approval number 2022-hs-77-02). Animal studies were approved by the Ethics Review Committee of Guangdong Provincial People's Hospital. (approval number KY-N-2021-070-01). Participants gave informed consent before taking part.

Provenance and peer review Not commissioned; externally peer reviewed.

Data availability statement Data are available upon reasonable request.

ORCID iDs
Lixue Cao http://orcid.org/0000-0002-0486-6587
Fei Yu http://orcid.org/0000-0003-1546-9365
Hui Zhang http://orcid.org/0000-0003-3620-610X
Xinxin Chen http://orcid.org/0009-0006-0846-8355

REFERENCES

1 Asleh K, Riaz N, Nielsen TO. Heterogeneity of triple negative breast cancer: Current advances in subtyping and treatment implications. *J Exp Clin Cancer Res* 2022;41:265.
2 Garrido-Castro AC, Lin NU, Polyak K. Insights into Molecular Classifications of Triple-Negative Breast Cancer: Improving Patient Selection for Treatment. *Cancer Discov* 2019;9:176–98.
3 Ademuyiwa FO, Gao F, Street CR, *et al*. A randomized phase 2 study of neoadjuvant carboplatin and paclitaxel with or without atezolizumab in triple negative breast cancer (TNBC) - NCI 10013. *NPJ Breast Cancer* 2022;8:134.
4 Rayson VC, Harris MA, Savas P, *et al*. The anti-cancer immune response in breast cancer: current and emerging biomarkers and treatments. *Trends Cancer* 2024;10:490–506.
5 Han Y, Xie W, Song D-G, *et al*. Control of triple-negative breast cancer using ex vivo self-enriched, costimulated NKG2D CAR T cells. *J Hematol Oncol* 2018;11:92.
6 Song D-G, Ye Q, Poussin M, *et al*. Effective adoptive immunotherapy of triple-negative breast cancer by folate receptor-alpha redirected CAR T cells is influenced by surface antigen expression level. *J Hematol Oncol* 2016;9:56.
7 Xie Y, Hu Y, Zhou N, *et al*. CAR T-cell therapy for triple-negative breast cancer: Where we are. *Cancer Lett* 2020;491:121–31.
8 Yang P, Cao X, Cai H, *et al*. The exosomes derived from CAR-T cell efficiently target mesothelin and reduce triple-negative breast cancer growth. *Cell Immunol* 2021;360:104262.
9 Zhang X, Guo H, Chen J, *et al*. Highly proliferative and hypodifferentiated CAR-T cells targeting B7–H3 enhance antitumor activity against ovarian and triple-negative breast cancers. *Cancer Lett* 2023;572:216355.
10 Byrd TT, Fousek K, Pignata A, *et al*. TEM8/ANTXR1-Specific CAR T Cells as a Targeted Therapy for Triple-Negative Breast Cancer. *Cancer Res* 2018;78:489–500.
11 Zhou M, Chen M, Shi B, *et al*. Radiation enhances the efficacy of EGFR-targeted CAR-T cells against triple-negative breast cancer by activating NF-κB/Icam1 signaling. *Mol Ther* 2022;30:3379–93.
12 Mardiana S, Solomon BJ, Darcy PK, *et al*. Supercharging adoptive T cell therapy to overcome solid tumor-induced immunosuppression. *Sci Transl Med* 2019;11:eaaw2293.
13 Stüber T, Monjezi R, Wallstabe L, *et al*. Inhibition of TGF-β-receptor signaling augments the antitumor function of ROR1-specific CAR T-cells against triple-negative breast cancer. *J Immunother Cancer* 2020;8:e000676.
14 Xia L, Zheng Z, Liu J-Y, *et al*. Targeting Triple-Negative Breast Cancer with Combination Therapy of EGFR CAR T Cells and CDK7 Inhibition. *Cancer Immunol Res* 2021;9:707–22.
15 Marinelli O, Nabissi M, Morelli MB, *et al*. ICOS-L as a Potential Therapeutic Target for Cancer Immunotherapy. *Curr Protein Pept Sci* 2018;19:1107–13.
16 Zhao X, Wang Y, Jiang X, *et al*. Comprehensive analysis of the role of ICOS (CD278) in pan-cancer prognosis and immunotherapy. *BMC Cancer* 2023;23:194.

17 Chen L, Flies DB. Molecular mechanisms of T cell co-stimulation and co-inhibition. *Nat Rev Immunol* 2013;13:227–42.
18 Mak TW, Shahinian A, Yoshinaga SK, *et al*. Costimulation through the inducible costimulator ligand is essential for both T helper and B cell functions in T cell–dependent B cell responses. *Nat Immunol* 2003;4:765–72.
19 Yamashita T, Tamura H, Satoh C, *et al*. Functional B7.2 and B7-H2 molecules on myeloma cells are associated with a growth advantage. *Clin Cancer Res* 2009;15:770–7.
20 Zhang Y, Luo Y, Qin S-L, *et al*. The clinical impact of ICOS signal in colorectal cancer patients. *Oncoimmunology* 2016;5:e1141857.
21 Conrad C, Gregorio J, Wang Y-H, *et al*. Plasmacytoid dendritic cells promote immunosuppression in ovarian cancer via ICOS costimulation of Foxp3(+) T-regulatory cells. *Cancer Res* 2012;72:5240–9.
22 Faget J, Bendriss-Vermare N, Gobert M, *et al*. ICOS-ligand expression on plasmacytoid dendritic cells supports breast cancer progression by promoting the accumulation of immunosuppressive CD4+ T cells. *Cancer Res* 2012;72:6130–41.
23 Guedan S, Chen X, Madar A, *et al*. ICOS-based chimeric antigen receptors program bipolar TH17/TH1 cells. *Blood* 2014;124:1070–80.
24 Shen C-J, Yang Y-X, Han EQ, *et al*. Chimeric antigen receptor containing ICOS signaling domain mediates specific and efficient antitumor effect of T cells against EGFRvIII expressing glioma. *J Hematol Oncol* 2013;6:33.
25 Wan Z, Shao X, Ji X, *et al*. Transmembrane domain-mediated Lck association underlies bystander and costimulatory ICOS signaling. *Cell Mol Immunol* 2020;17:143–52.
26 Fauci JM, Sabbatino F, Wang Y, *et al*. Monoclonal antibody-based immunotherapy of ovarian cancer: targeting ovarian cancer cells with the B7-H3-specific mAb 376.96. *Gynecol Oncol* 2014;132:203–10.
27 Du H, Hirabayashi K, Ahn S, *et al*. Antitumor Responses in the Absence of Toxicity in Solid Tumors by Targeting B7-H3 via Chimeric Antigen Receptor T Cells. *Cancer Cell* 2019;35:221–37.
28 Liu B, Zou F, Lu L, *et al*. Chimeric Antigen Receptor T Cells Guided by the Single-Chain Fv of a Broadly Neutralizing Antibody Specifically and Effectively Eradicate Virus Reactivated from Latency in CD4+ T Lymphocytes Isolated from HIV-1-Infected Individuals Receiving Suppressive Combined Antiretroviral Therapy. *J Virol* 2016;90:9712–24.
29 Sanjana NE, Shalem O, Zhang F. Improved vectors and genome-wide libraries for CRISPR screening. *Nat Methods* 2014;11:783–4.
30 Ba H, Dai Z, Zhang Z, *et al*. Antitumor effect of CAR-T cells targeting transmembrane tumor necrosis factor alpha combined with PD-1 mAb on breast cancers. *J Immunother Cancer* 2023;11:e003837.
31 Sanmamed MF, Rodriguez I, Schalper KA, *et al*. Nivolumab and Urelumab Enhance Antitumor Activity of Human T Lymphocytes Engrafted in Rag2-/-IL2Rγnull Immunodeficient Mice. *Cancer Res* 2015;75:3466–78.
32 Wang Z, Yu Y, Dai W, *et al*. A specific peptide ligand-modified lipid nanoparticle carrier for the inhibition of tumor metastasis growth. *Biomaterials* 2013;34:756–64.
33 Tian Q, Gao H, Zhou Y, *et al*. RICH1 inhibits breast cancer stem cell traits through activating kinases cascade of Hippo signaling by competing with Merlin for binding to Amot-p80. *Cell Death Dis* 2022;13:71.
34 Yoshinaga SK, Whoriskey JS, Khare SD, *et al*. T-cell co-stimulation through B7RP-1 and ICOS. *Nature New Biol* 1999;402:827–32.
35 Leconte J, Bagherzadeh Yazdchi S, Panneton V, *et al*. Inducible costimulator (ICOS) potentiates TCR-induced calcium flux by augmenting PLCγ1 activation and actin remodeling. *Mol Immunol* 2016;79:38–46.
36 Liakou CI, Kamat A, Tang DN, *et al*. CTLA-4 blockade increases IFNgamma-producing CD4+ICOShi cells to shift the ratio of effector to regulatory T cells in cancer patients. *Proc Natl Acad Sci U S A* 2008;105:14987–92.
37 Chen H, Liakou CI, Kamat A, *et al*. Anti-CTLA-4 therapy results in higher CD4+ICOShi T cell frequency and IFN-gamma levels in both nonmalignant and malignant prostate tissues. *Proc Natl Acad Sci U S A* 2009;106:2729–34.
38 Fan X, Quezada SA, Sepulveda MA, *et al*. Engagement of the ICOS pathway markedly enhances efficacy of CTLA-4 blockade in cancer immunotherapy. *J Exp Med* 2014;211:715–25.
39 Hilton JF, Ott PA, Hansen AR, *et al*. INDUCE-2: A Phase I/II, open-label, two-part study of feladilimab in combination with tremelimumab in patients with advanced solid tumors. *Cancer Immunol Immunother* 2024;73:44.
40 Hou AJ, Chen LC, Chen YY. Navigating CAR-T cells through the solid-tumour microenvironment. *Nat Rev Drug Discov* 2021;20:531–50.
41 Simpson TR, Quezada SA, Allison JP. Regulation of CD4 T cell activation and effector function by inducible costimulator (ICOS). *Curr Opin Immunol* 2010;22:326–32.
42 Choi YS, Kageyama R, Eto D, *et al*. ICOS receptor instructs T follicular helper cell versus effector cell differentiation via induction of the transcriptional repressor Bcl6. *Immunity* 2011;34:932–46.
43 Peng C, Huggins MA, Wanhainen KM, *et al*. Engagement of the costimulatory molecule ICOS in tissues promotes establishment of $CD8^+$ tissue-resident memory T cells. *Immunity* 2022;55:98–114.
44 Le K-S, Amé-Thomas P, Tarte K, *et al*. CXCR5 and ICOS expression identifies a CD8 T-cell subset with T_{FH} features in Hodgkin lymphomas. *Blood Adv* 2018;2:1889–900.
45 Khanam A, Tang LSY, Kottilil S. Programmed death 1 expressing $CD8^+$ $CXCR5^+$ follicular T cells constitute effector rather than exhaustive phenotype in patients with chronic hepatitis B. *Hepatology* 2022;75:690–708.
46 Agarwal S, Hanauer JDS, Frank AM, *et al*. In Vivo Generation of CAR T Cells Selectively in Human CD4+ Lymphocytes. *Mol Ther* 2020;28:1783–94.
47 Boulch M, Cazaux M, Cuffel A, *et al*. Tumor-intrinsic sensitivity to the pro-apoptotic effects of IFN-γ is a major determinant of $CD4^+$ CAR T-cell antitumor activity. *Nat Cancer* 2023;4:968–83.
48 Nelson MH, Knochelmann HM, Bailey SR, *et al*. Identification of human $CD4^+$ T cell populations with distinct antitumor activity. *Sci Adv* 2020;6:eaba7443.
49 Boulch M, Cazaux M, Loe-Mie Y, *et al*. A cross-talk between CAR T cell subsets and the tumor microenvironment is essential for sustained cytotoxic activity. *Sci Immunol* 2021;6:eabd4344.
50 Liadi I, Singh H, Romain G, *et al*. Individual Motile CD4(+) T Cells Can Participate in Efficient Multikilling through Conjugation to Multiple Tumor Cells. *Cancer Immunol Res* 2015;3:473–82.
51 Burugu S, Dancsok AR, Nielsen TO. Emerging targets in cancer immunotherapy. *Semin Cancer Biol* 2018;52:39–52.
52 Solinas C, Gu-Trantien C, Willard-Gallo K. The rationale behind targeting the ICOS-ICOS ligand costimulatory pathway in cancer immunotherapy. *ESMO Open* 2020;5:e000544.
53 Fos C, Salles A, Lang V, *et al*. ICOS ligation recruits the p50alpha PI3K regulatory subunit to the immunological synapse. *J Immunol* 2008;181:1969–77.
54 Leavenworth JW, Verbinnen B, Yin J, *et al*. A p85α-osteopontin axis couples the receptor ICOS to sustained Bcl-6 expression by follicular helper and regulatory T cells. *Nat Immunol* 2015;16:96–106.